

CHAPTER SIX

RESULTS

6.1 INTRODUCTION

This chapter presents the results of the investigation of microstructure, chemical composition and phase analysis of Smorgon Steel Works dust using SEM, diagnostic leaching and XRD. The SEM results of the Smorgon Steel Works feed dust are contained in Section 6.2 as well as the chemical composition and phase analysis. The laboratory experiments on the iron-reduction distillation process are divided into two sections. The first reduction stage results and the second reduction stage results which were carried out in a nitrogen atmosphere and under vacuum are presented in Sections 6.3 and 6.4 respectively.

6.2 CHARACTERISATION OF SMORGON STEEL WORKS DUST

The study of characterisation of Smorgon Steel Works dust is based on SEM analysis, diagnostic leaching and XRD analysis. From the SEM analysis the microstructure of EAF dust was obtained. Phase analysis was obtained from XRD and the concentrations of the common phases were carried out by diagnostic leaching.

6.2.1 Microstructure

The SEM (Figure 6.1-6.3) showed that the Smorgon Steel Works dust particles are generally less than five microns in size, while most of the particles are less than one micron. Some of the particles are less than half of a micron. The particles are predominantly spherical. The SEM-EDS indicated that the spherical particles are iron oxide as shown in Figure 6.3. The spherical light gray particle (at point 1 of high magnification, Figure 6.3) which has a diameter of about 48 microns is an iron oxide particle. The EDS result showed that this particle contained 70.85%Fe and 28.26%O by weight indicating that this particle is magnetite. Zinc oxide occurs as dark gray phase (at point 2 of high magnification, Figure 6.3). The EDS result showed that this particle contained 79.66%Zn and 18.73%O by weight.

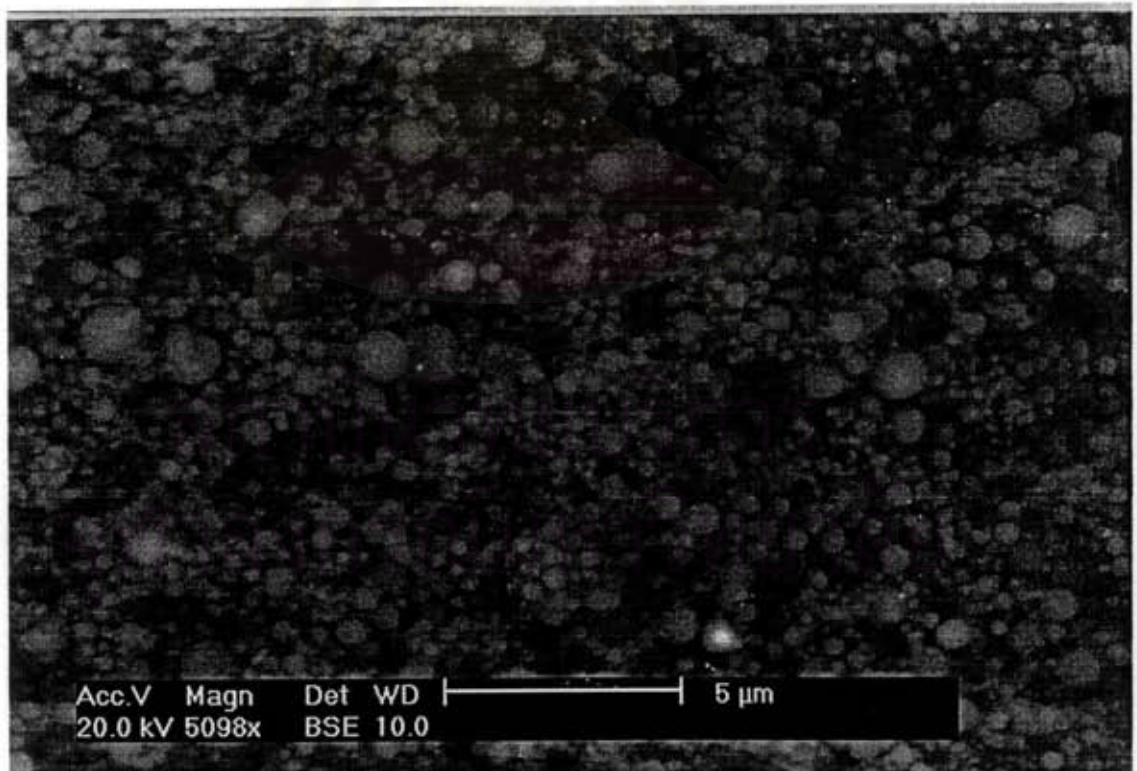


Figure 6.1: Photomicrograph showing EAF Dust particles.

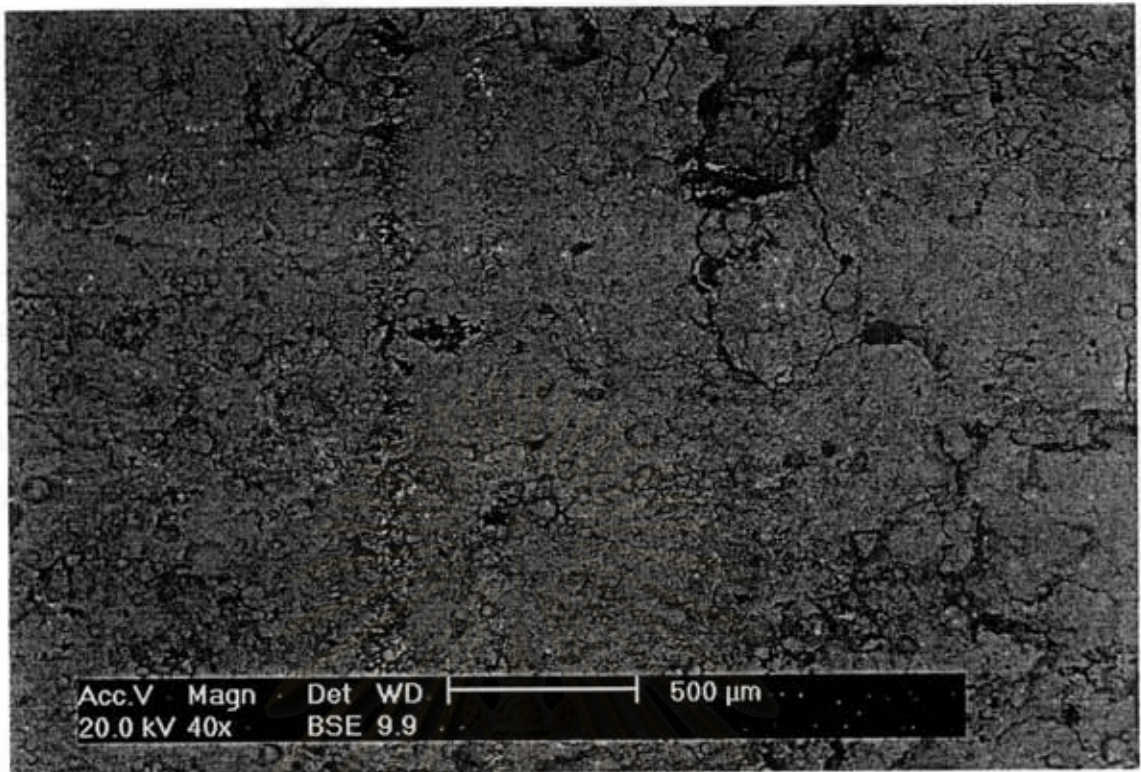


Figure 6.2: Photomicrograph showing EAF Dust particles.

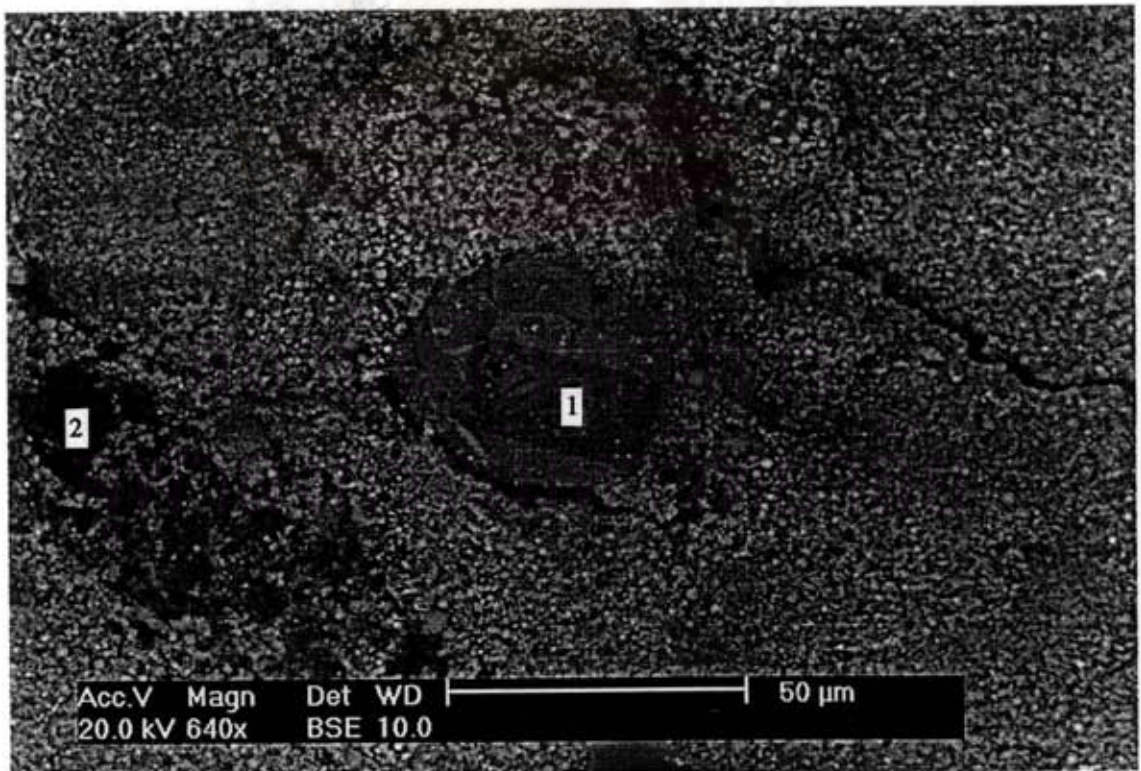


Figure 6.3: 1) Magnetite (light gray) sphere (about 48 micron-diameter), 2) Zinc oxide (dark gray).

6.2.2 Chemical Composition

The concentration of elements contained in the EAF dusts obtained from Smorgon Steel Works is present in Table 6.1. The EAF dusts were generated during March 1998. The major elements in the dusts are zinc and iron. The compounds formed from the zinc and iron accounts for approximately 70% by weight of the dusts. In addition, the dusts contain significant quantities of alkaline elements, such as sodium and potassium, and halide, such as chlorine. Hazardous elements, such as lead, cadmium and chromium also occurred.

Table 6.1: Elemental Composition of Smorgon Steel Works Dusts
(Table obtained from Smorgon Steel Works).

Element	Concentration (wt%)
Iron (Fe)	22.24-43.03
Zinc (Zn)	17.47-38.70
Lead (Pb)	1.09-3.81
Cadmium (Cd)	0.021-0.15
Arsenic (As)	0.003-0.13
Copper (Cu)	0.07-0.21
Manganese (Mn)	1.73-2.08
Chromium (Cr)	0.10-0.23
Nickel (Ni)	0.01-0.12
Calcium (Ca)	2.97-5.14
Sodium (Na)	0.29-2.31
Potassium (K)	0.70-2.34
Chlorine (Cl)	0.93-5.61
Sulphur (S)	0.84-3.23
Silicon (Si)	0.80-1.04

Table 6.2 shows the concentration of elements of EAF dust generated at the Smorgon Steel Works and used in this study.

Table 6.2: Elemental Composition of Unreacted EAF Dust Generated at the Smorgon Steel Works and Used in this Study.

Element	Concentration (wt%)
Iron (Fe)	37.20
Zinc (Zn)	19.20
Lead (Pb)	1.52
Cadmium (Cd)	0.021
Arsenic (As)	0.003
Chromium (Cr)	0.19
Nickel (Ni)	0.02
Molybdenum (Mo)	0.02
Manganese (Mn)	1.73
Magnesium (Mg)	0.82
Copper (Cu)	0.17
Calcium (Ca)	4.21
Sodium (Na)	0.88
Potassium (K)	0.73
Chlorine (Cl)	0.93
Silicon Dioxide (SiO ₂)	3.44

The elemental composition of EAF dust sample were checked by Spectrometer Services PTY.LTD., Coburg, Melbourne, Australia by the inductively coupled plasma atomic emission spectroscopy (ICP-AES) method.

6.2.3 Phase Analysis

XRD analysis of Smorgon Steel Works dust showed that the dominant phases are a spinel group present as zinc ferrite ($\text{ZnO}\cdot\text{Fe}_2\text{O}_3$) and magnetite (Fe_3O_4) but it cannot distinguish between these two phases. Another form of zinc is present as zinc oxide. The halide group are present as sodium chloride (NaCl) and potassium chloride (KCl). Lime (CaO) was also detected by XRD. The XRDPs of the unreacted EAF dust are shown in Figure D1 of Appendix D. Table 6.3 shows the estimated concentration of the common compounds in Smorgon Steel Works dust used in this study obtained by diagnostic leaching. XRD analysis was also used to determine the residues obtained after leaching.

Table 6.3: Estimated Concentration of the Common Compounds in Smorgon Steel Works Dust Used in this Study.

Compounds / Spinel	Concentration (wt%)
Zinc Oxide (ZnO)	7.80
Zinc Ferrite ($\text{ZnO}\cdot\text{Fe}_2\text{O}_3$)	40.96
Magnetite (Fe_3O_4)	24.49
Sodium Chloride (NaCl) and Potassium Chloride (KCl)	4.45

The halides are soluble in hot water. After filtration, the solution was evaporated. The XRDPs of the solid residue are shown in Figure D2 of Appendix D. From XRD analysis it was found that only NaCl and KCl were leached by this method and no halide peaks were found in the EAF dust after hot water leaching. Figure D3 of Appendix D shows the XRDPs of EAF dust after hot water leaching. Zinc oxide could be dissolved in dilute sulphuric acid and formed zinc sulphate. Figure D4 of Appendix D shows the XRDPs of EAF dust after dilute sulphuric acid leaching. The zinc oxide peaks have decreased.

6.3 FIRST REDUCTION STAGE RESULTS

In this study, two types of briquettes were used in the experiments. For Run series A, B, C, and D the reduction was carried out using non-sintered briquettes. For Run series E reduction was carried out using sintered briquettes. In this stage, the effect of temperature and time, reduction gas composition and sintering process were investigated.

The experimental results with the CO/CO₂ gas ratio of 9 at temperatures 600 to 800°C are shown in Figure 6.4 .

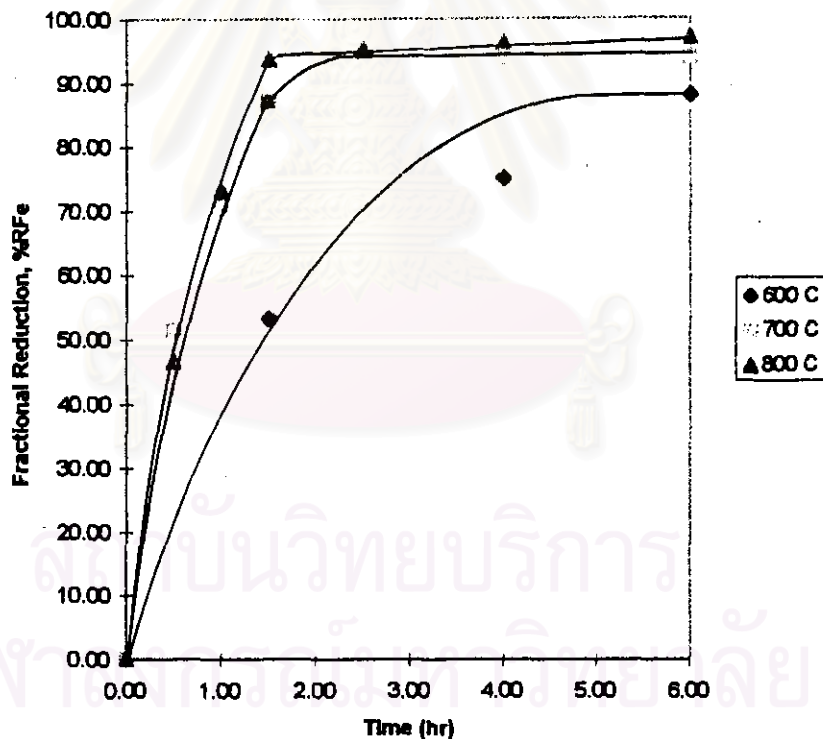


Figure 6.4: Results of the first reduction stage for EAF dust with CO/CO₂ gas ratio of 9 .

Magnetite in the feed dust was reduced by carbon monoxide to metallic iron in two and a half to three hours at 700 and 800 °C. Zinc ferrite also was reduced by carbon monoxide and produced zinc oxide and metallic iron. The solid residue of the reduced briquette was examined by XRD for analysis of the phases. The XRDPs in Figure D5 of Appendix D shows zinc oxide, metallic iron, wustite and some cementite peaks in the reduced briquette.

The elemental composition analysis of the reduced briquette was carried out using the ICP-AES method by Spectrometer Services PTY.LTD. Table 6.4 shows the elemental composition of reduced briquette compared with the feed dust.

The results obtained from Spectrometer Services PTY.LTD. are shown in Appendix G as well as the mass balance calculation given in Table 6.4 and Table 6.5 . The results in both tables (Table 6.4 and 6.5) were based on 100 g feed.

From Table 6.4, it can be seen that about 0.65 percent of zinc oxide was reduced by carbon monoxide at 700 °C. Cadmium oxide in the feed dust also was reduced by carbon monoxide and evaporated.

Table 6.4: Elemental Composition (wt%) of the EAF Dust and the Residue after the First Reduction Stage.

Dust Type	Conditions	Zn	Fe	Cd	Pb	Na	K	Cl	Cr
Feed EAF dust	unreacted	19.20	37.20	0.021	1.52	0.88	0.73	0.93	0.19
Residue after reduction	CO/CO ₂ =9, 700 °C, reduction time 2.5 hrs	18.55	37.20	<18 ppm	1.50	0.85	0.65	1.14	0.19

Figure 6.5 shows the effect of gas composition on the first reduction stage at 700 °C. The larger CO/CO₂ gas ratio gave a faster reduction rate of magnetite and zinc ferrite.

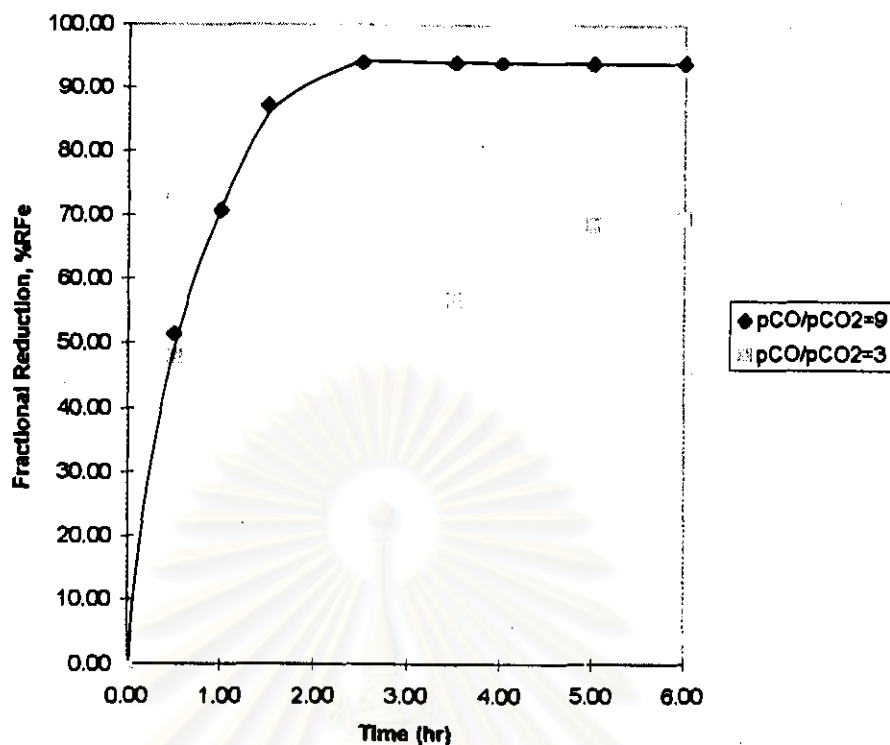


Figure 6.5: Effect of CO/CO₂ gas composition on the first reduction stage rates at 700°C.

Figure 6.6 shows the effect of the sintering process on the first reduction stage rates at 700 °C. These briquettes were fired in a muffle furnace in air for 24 hours at 1100 °C. The heating rate from room temperature to 1100 °C was 100 °C per hour and cooling was at the same rate to room temperature before removal. From XRD, it was found that the major phases after firing were zinc ferrite and magnetite. Little zinc oxide phase was present after firing. The XRDPs of the unreacted sintered briquette are shown in Figure D6 of Appendix D.

For the sintered briquette most of the zinc content was in the form of zinc ferrite. Figure 6.6 shows that the reduction rates of the sintered briquette was lower than the non-sintered briquette in the first two and a half hours but after that the reduction rates were quite similar.

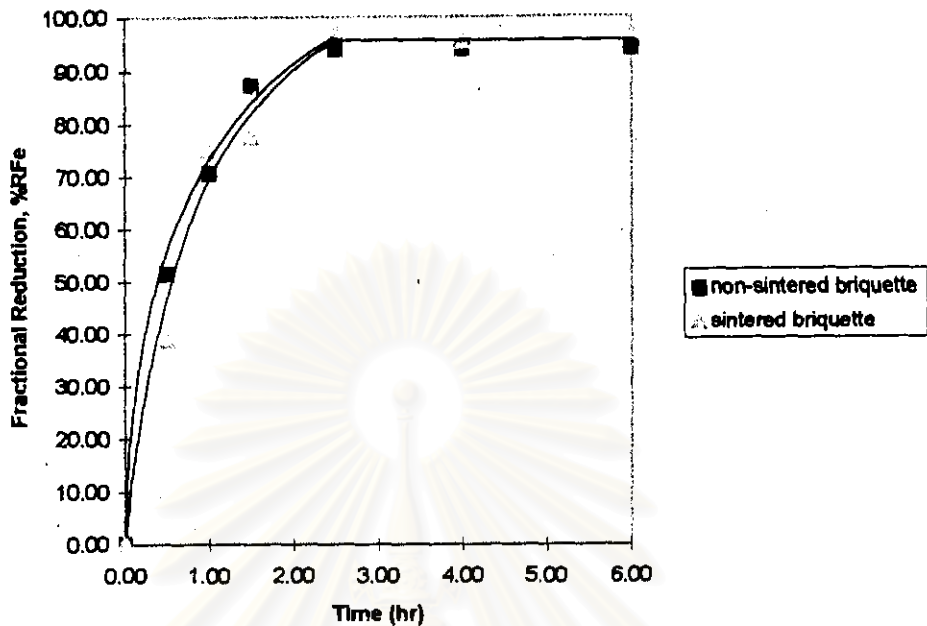


Figure 6.6: Effect of sintering process on the first reduction stage rates at 700 °C and CO/CO₂ gas ratio of 9 .

The results show that for the first reduction stage, temperatures between 700 and 800°C with a CO/CO₂ gas ratio of 9 are suitable because under these conditions about 94 to 97 percent reduction of metallic iron was obtained and would be used to reduce zinc oxide in the second reduction stage.

สำนักงานวิทยบริการ
จุฬาลงกรณ์มหาวิทยาลัย

6.4 SECOND REDUCTION STAGE RESULTS

Reduced briquette samples from the first reduction stage were used in these experiments. The non-sintered briquette samples were reacted at 700 °C, CO/CO₂ gas ratio of 9 for two and a half hours reduction time. From Section 6.3, it was shown that under these condition about 94.0 wt% metallic iron was produced. The metallic iron was used to reduce zinc oxide in the second reduction stage. Experiments were carried out in a nitrogen atmosphere and under vacuum so as to compare the rates of reduction of zinc oxide by metallic iron to zinc vapour.

6.4.1 In Nitrogen Atmosphere

In this system, zinc vapour produced from the reaction was removed from the reaction furnace by nitrogen gas.

Figure 6.7 shows the results of the zinc oxide reduction at 900 to 1200 °C. The vertical axis labeled R_{Zn} shows the zinc reduction ratio based on the mass loss of the samples. The reaction rate increased as the temperature increased. All of the zinc was reduced within 30 minutes at 1200°C. On the other hand, when the temperature used was 900°C, the maximum zinc reduction was only 87.59% and reduction rate was very slow. The maximum variation in the percent reduction between the two runs at 900, 1000, 1100 and 1200 °C were 26.68, 1.20, 3.78 and 8.26 percent, respectively. All of the raw data of two curves of each temperature are presented in Appendix F. The presented results were obtained from the mean value of the two curves.

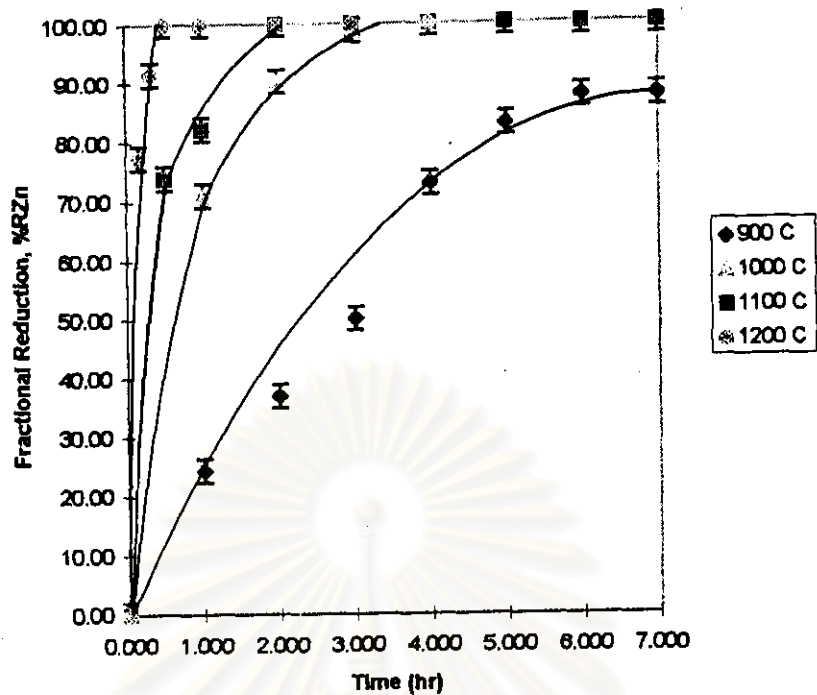


Figure 6.7: Results of the second reduction stage in a nitrogen atmosphere.

6.4.2 Under Vacuum

A vacuum of 2.0×10^{-3} atm was used to remove zinc vapour from the reaction furnace.

Figure 6.8 shows the results of the second reduction stage in vacuum at 800 to 1000 °C. The reaction proceeded very fast under vacuum of 2.0×10^{-3} atm as the temperature was increased. For example, all of the zinc oxide was reduced and distilled within 40 minutes at 1000 °C. At the same temperature, in a nitrogen atmosphere the reduction rate was very slow as shown in the Figure 6.9 . At 1000 °C, all of the zinc oxide was reduced within 40 minutes under vacuum but required 4 hours in a nitrogen atmosphere. The maximum variation in the percent reduction between the two runs at 800, 900 and 1000 °C were 5.48, 2.86 and 3.52 percent, respectively. All of the raw data of two curves of each temperature are presented in Appendix G. The presented results were obtained from the mean value of the two curves.

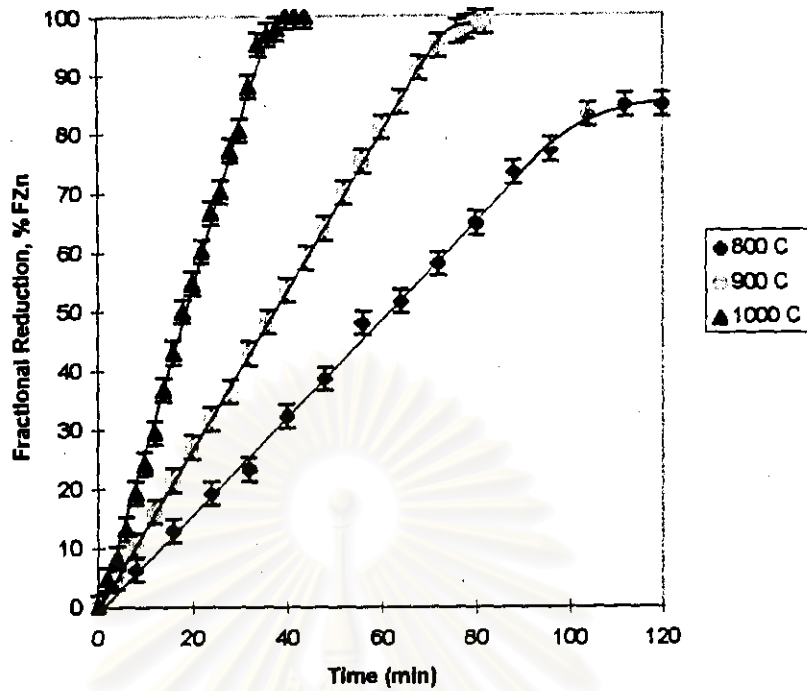


Figure 6.8: Results of the second reduction stage under vacuum.

สถาบันวิทยบริการ
จุฬาลงกรณ์มหาวิทยาลัย

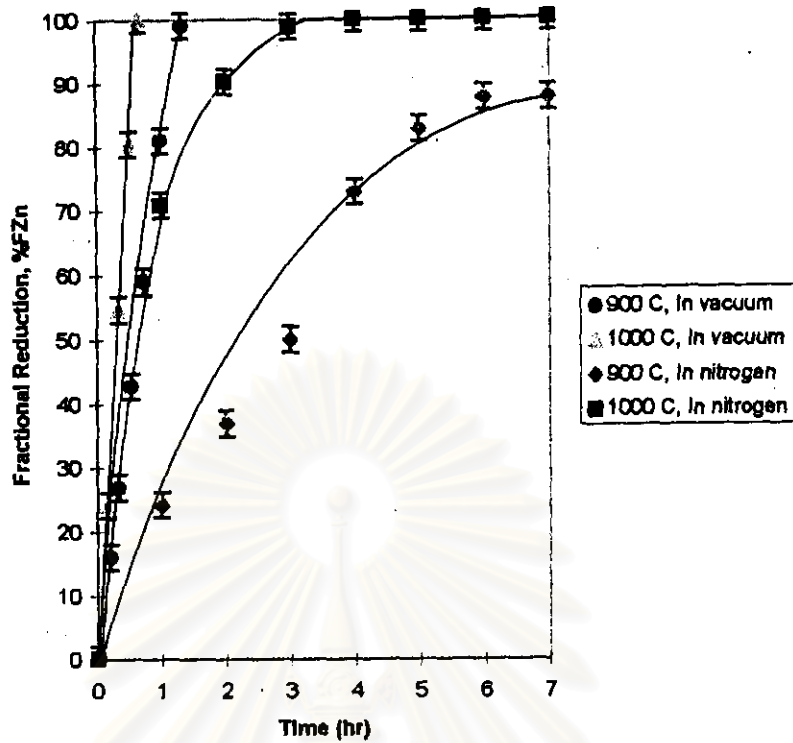


Figure 6.9: Effect of nitrogen atmosphere and under vacuum on the second reduction stage rates at 900 and 1000 °C.

สถาบันวิทยบริการ
จุฬาลงกรณ์มหาวิทยาลัย

The solid residues were examined by XRD for phase analysis. Both XRDPs in Figure D7 (in nitrogen) and D8 (under vacuum) of Appendix D show that the wustite and metallic iron are the major phases obtained after the second reduction stage. Some hematite and magnetite peaks are also present but all peaks are low intensity. No zinc oxide peaks were present in both XRD results.

The elemental composition of reduced briquettes were carried out using ICP-AES by Spectrometer Services PTY.LTD. Table 6.5 shows the elemental composition of reduced briquettes compared with the feed dust.

Table 6.5 shows that the percentage of zinc decreased after reduction in both nitrogen atmosphere and under vacuum. The percentage of cadmium was the same as the residue obtained from the first reduction stage. Lead, sodium, potassium and chlorine levels clearly decreased after reduction in both nitrogen atmosphere and under vacuum.

Table 6.5: Elemental Composition (wt%) of the EAF Dust and the Residues after the Second Reduction Stage.

Dust Type	Conditions	Zn	Fe	Cd	Pb	Na	K	Cl	Cr
Feed EAF dust	unreacted	19.20	37.20	0.021	1.52	0.88	0.73	0.93	0.19
2 nd reduction in N ₂ atmosphere	900 °C, 7 hrs	4.85	37.20	<18 ppm	0.46	N/A	N/A	N/A	N/A
2 nd reduction in N ₂ atmosphere	1200 °C, 4 hrs	0.38	37.20	<18 ppm	0.47	0.25	<60 ppm	<60 ppm	0.19
2 nd reduction in vacuum system	1000 °C, 28 mins	3.77	37.20	<18 ppm	67 ppm	0.07	0.014	<67 ppm	0.19

The polished cross section of the reduced briquettes were analysed by the SEM-EDS. EDS analyses were carried out on nitrogen atmosphere and vacuum reduced briquettes in order to verify the zinc level. The analyses were performed at various positions from the centre of the briquette to the outside edge. The briquettes were reacted for 3 hours at 900 °C in nitrogen and for 20 minutes at 1000 °C under vacuum. The zinc fractional reduction for both samples was about 50 to 60% . The results are shown in Figure 6.10 .

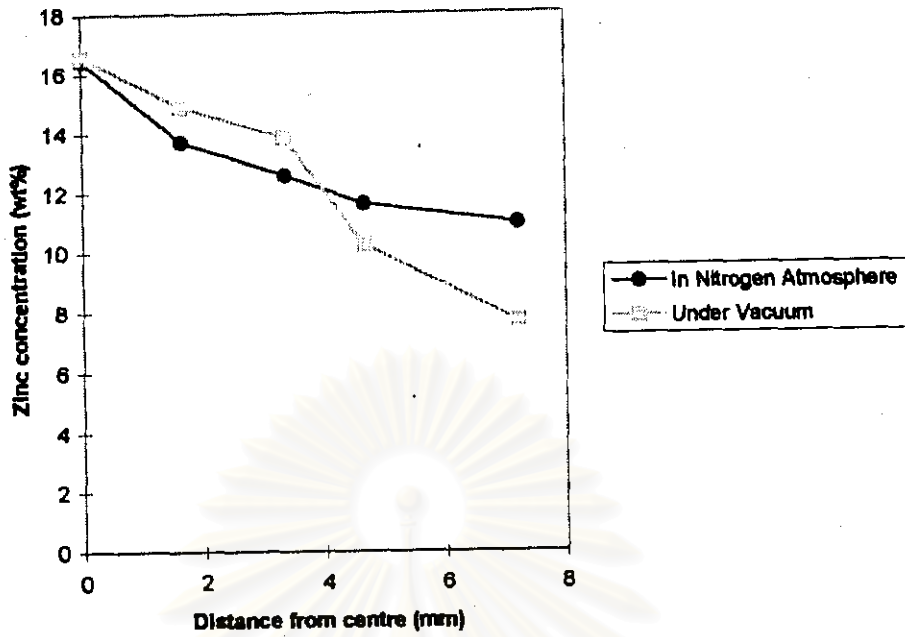


Figure 6.10: The EDS analysis of zinc level at various positions on the briquette surfaces.

Figure 6.10 shows that the zinc concentration decreases from the centre to the edge of the briquette for both samples (in nitrogen atmosphere and under vacuum).

สถาบันวิทยบริการ
จุฬาลงกรณ์มหาวิทยาลัย